International Research Journal of Multidisciplinary Scope (IRJMS), 2024; 5(3):559-570

Original Article | ISSN (O): 2582-631X DOI: 10.47857/irjms.2024.v05i03.01007

Compact Multiband CP Filtering Antenna for Bandwidth Enhancement

Kiran Hilal Sonawane*, Pravin Sahebrao Patil

Department of Electronics and Telecommunication, SSVPSBS Deore College of Engineering, Dhule, Maharashtra, India. *Corresponding Author's Email: khsona2009@gmail.com

Abstract

A miniature circularly polarized filtering antenna device is presented here. The device consists of circular radiating patch impeccably coupled using pins to strip line circuits having open loop ring resonators. In proposed design the last stage of filter acts as radiating patch and having low profile of size 0.57λ0 x 0.57λ0 x 0.07λ0 at center frequency 4.26GHz. Filtering circuit improves wide impedance bandwidth and axial ratio 3dB bandwidth. It gives a deep null at upper and lower band edges of filter response. The CP version develops from two LP design by introducing a T-shaped near-field resonant parasitic element near the probe to create two transmission paths with an inherent 90° phase difference. The filtenna is design, fabricated and measured having gain more than 2.5dB and reflection coefficient (S_{11}) < -14dB for an impedance bandwidth of 580MHz from 4.06 to 4.64GHz. Fractional bandwidth, which is 13.33%, gives good candidature for variety of wireless applications. The developed circularly polarized co-design filtering antenna is verified using full wave models and testing. The filtering antenna is useful for biomedical applications such as wearable devices and 5G applications.

Keywords: Circularly Polarized, Compact Antennas, Filtennas, Linearly Polarized Antennas, Low Profile.

Introduction

The integration of microwave components has become necessary where size reduction and increased overall performance are concerned as wireless communication technology is improving day by day. Any antenna design requires both antenna and filter circuits, which are vital elements in design process. A hybrid feeding methodology with integrated strip line and air filled substrate waveguide structures is employed to create a circularly polarized antenna array (1). In the other study (2), a small footprint single layer circularly polarized patch antenna is built. Wideband circularly polarized 2x2 filtenna was obtained in a study (3) with increased gain and AR bandwidth. Signal transmission and reception are handled by the antenna, while the frontend circuit known as band pass filter is in charge of separation of desired signal. The quality of the S_{11} and gain of antenna is impaired by interference since the antenna and BPF are resonating at the same frequency. If the impedance is not correctly synched, the enactment of antenna will be adversely impacted, for example by 50 or 75Ω over the bandwidth or at the band edges. Recent work has focused on code sign BPF and antenna into a single device. The ultimate solution is provided by the final stage of filter design, which behaves as an antenna radiator as electromagnetic bandgap antenna (4). To acquire good bandwidth, several filtering antennas was studied. In several existing literature, antennas were used as dispersive complex loads in filter circuits for horn antennas (5, 6), wire monopoles (7), coupled planar resonator connected patch antenna (8, 9), SIW resonator with coaxial collinear antennas (10). In code sign, last stage of BPF acts as antenna having coupled substrate-integrated waveguide cavity filters cascaded to slot antennas (11-13) and planar monopole antennas combined with coupled line filters (14-16). A filtenna is 40mm x 40mm x 5.3mm is compared with other filtering antenna in Table 2. Due to their applications in wireless communications, which hold enormous potential for bio-medical fields, battlefield survival,

(Received 26th April 2024; Accepted 15th July 2024; Published 30th July 2024)

and patient tracking systems. Wearable antenna one of the fastest-evolving fields in the antenna community, has attracted research interest from all over the world (17, 18). Different types of wearable antennas were developed on HSCA and PICA (19), IFA (20), planer micro-strip monopoles (21-23), PIFA (24, 25), slot antennas (26), stepped impedance resonator antenna (27), patch antennas (28), cavity backed slot antenna (29, 30) having broadside radiation pattern. Artificial magnetic conducting surfaces (31-33) and meta-surface (34) having small isolation profile between antenna and human tissues.

Narrow operating band and polarization operations are the two main issues, we address in this research by introducing an innovative design approach for compact CP filtenna without adjusting the size of antenna. This multilayer filtenna, not only increased impedance bandwidth but also creates two deep radiation nulls that improves out of band rejection of filter performance. In the methodology section, we described the design of circularly polarized filtenna by elucidating 3D design, equivalent circuit, and structural design of module. Also compare final ring resonator with other two design antennas. In results and discussion section describes the simulation and measurement outcomes in air, compared with other existing antennas and finally discuss conclusion and future scope of design.

Methodology

The prototype of co-design CP filtenna is portrayed in Figure 1 having circular patch radiator on top layer, and a planer dual strip-line microwave circuit on middle layer consisting of filtering, phase splitting, power disparities and conjugate matching functions required to radiate CP wave. The filter circuit is sandwiched in between ground plane and radiating circular plane which increase impedance bandwidth. With this configuration, size of whole device can be significantly reduced. The impedance at interferences is optimized by adjusting the location and dimension of via hole to attain better performance. For proposed design, we are replacing rectangular open loop resonator with open loop ring resonator. Two bandpass filters are connected to circular radiating patch through coupled strip-line and two metallic pins that pass-through ground plane in between top and middle layers. The two metallic pins are located at some offset from center of circular radiating patch to obtain a good impedance matching. The bottom ground plane of circular patch radiator (top layer) acts as top ground plane of strip-line circuit (middle layer). Two bandpass filter circuits consist of three open-loop ring resonators which are mutually coupled to one another. Subminiature version A (SMA) connector is connected to bandpass filter with top and bottom ground connected from side instead of bottom side, as discussed in wearable medical uses (35, 36). The size of filtenna is 40mm x 40mm x 5.3mm (0.57 λ_L x 0.57 λ_L x 0.07 λ_L) where λ_L =70.42mm, which is compact as compared to other filtering antennas compared in Table 2. To satisfy criteria mentioned above, a ring resonator multi-layer filtering antenna array has been chosen. A RT/Duroid 5880 with the dielectric constant ε_r =2.2, thickness of substrate 0.79mm, loss tangent tanδ =0.0009 and copper layer thickness 18μm is used for prototype design. A radius of patch is only parameter to control the resonant frequency. Radius of patch (a) can be determined by

$$a = \frac{F}{\sqrt{\left\{1+\left(\frac{2h}{\pi\varepsilon_{rF}}\right)\lfloor ln ln\left(\frac{\pi F}{2h}\right)+1.7726\rfloor\right\}}} \quad \text{----------[1]}$$

Where $$F = \frac{8.791\times10^9}{f_r\sqrt{\varepsilon_r}} \quad \text{---------[2]}$$

The radius of patch is calculated by substituting h= 3.68mm, ε_r = 2.2, F=1.4817 in equation 1, the computed value of radius (a) is 1.477cm=14.77mm, h is height of substrate, ε_r = dielectric constant of substrate. The layout is represented in Figure 1, where three substrate layers have height h_1=3.68, h_2=0.79, h_3=0.79 all in millimeters. The analogous circuit for CP filtenna is publicized in Figure 2. A shunt equivalent circuit (Rx, Lx, Cx or Ry, Ly, Cy) was used for orthogonal model. The inductance of the feeding pin is represented by a series inductor. The three parallel RLC resonators represent three open loop ring resonators (OLRR), which can be synchronously/asynchronously tuned (37). An admittance inverter is used to couple stages (38). Coupled strip lines are capacitively coupled, third resonators are connected to for circular radiating patch as a part of integrated filter design (39). For circular polarization, two filtering branches are attached to T section having an electrical length of λ/4 for impedance matching and also giving 90° phase difference.

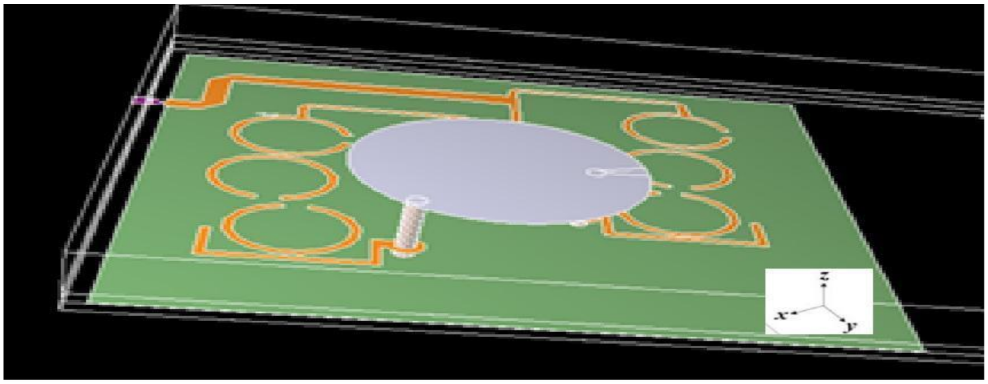

Figure 1: 3D View of CP Filtenna Using Open Loop Ring Resonator

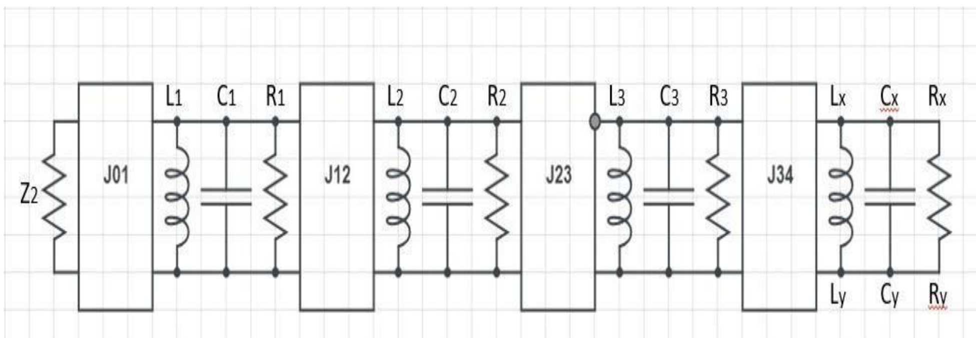

Figure 2: Equivalent Circuit of CP Filtenna

The prototype antenna has quarter order Chebyshev BPF, of fc= 4.26GHz, S_{11}= 13.33% and a 50Ω impedance. At the T-shaped junction, two branches converge has feed patch with quadrature phase between them to realize circular polarization. A ʎ/4 (quarter-wave transformer) is formed to synch impedance of 50Ω at antenna port. Two BPFs are designed so that bandwidth should be enhanced with filtering and impedance matching functions (40). The Chebyshev fourth order LPF prototype elements values with a ripple factor of 0.2dB were got as g0=1.0, g1=1.303, g2=1.284, g3=1.976, g4=0.847, g5=1.539.

For low pass normalization, to get the actual component values the following equations are used,

$$C_n = \frac{G_n}{2\pi f_c R} \quad \text{-------------[3]}$$

$$L_n = \frac{G_n R}{2\pi f_c} \quad \text{--------------[4]}$$

Using equation 3 & 4 we can find values of C1=0.608pf, C2=0.599pf, C3=0.922pf, L1=3.89nH, L2=3.83nH, L3=5.90nH, R1=R2=R3=0.649Ω, Z_{BPFi}=Z_2=80Ω. The AR should stay below 3dB throughout this 13.33% impedance bandwidth. The antenna is last stage of resonator of filter acts as circular patch radiator. The resistance of each BPF acts as purely resistive. Based on the low-pass parameters, the design parameters of the band-pass can be calculated as below.

The external quality factors,

$$Q_{e1} = \frac{g_0 g_1}{FBW}, \quad Q_{en} = \frac{g_n g_{n+1}}{FBW} \quad \text{---------------[5]}$$

$$Q_e = \frac{g_1}{FBW} = \frac{1.303}{0.1333} = 9.774 \quad \text{---------------[6]}$$

Coupling coefficients for filters, can be determined by,

$$M_{i,i+1} = M_{n-i,n-i+1} = \frac{FBW}{\sqrt{g_i g_{i+1}}}\ for\ i = 1,2, \ldots\ldots, \frac{n}{2} - 1 \quad \text{---------------[7]}$$

$$M_{12} = M_{34} = \frac{0.1333}{\sqrt{1.303 \times 1.284}} = 0.090$$

And $M_{i,n+1-i} = \frac{FBW.J_i}{g_i}\ for\ i = 1,2, \ldots \ldots, \frac{n}{2}$ ---------------[8]

$$M_{23} = \frac{0.1333 \times 0.8012}{1.284} = 0.083$$

Where Qe1 and Qen are the external quality factors of the resonators at the input and output port and Mi,i+1 is coupling coefficients between i^{th} and $(i+1)^{th}$ resonator, n is order of filter. Consider electrical length of ʎ/4 at fc and characteristic impedance of 80Ω to obtain desired performance. At center frequency, the coupled strip-line's length should be approximately one-quarter wavelength is 12.6mm. The separation distance was determined to be 0.21mm. Wide bandwidth is obtained by using two LPFs joined to T junction. The two planer strip lines have a length difference of around 12.6mm which is ʎ/4 of fc. Over 13.33% bandwidth, a quarter wavelength strip-line provides desired 90° phase shift. A quarter wave transformer is used for impedance matching of input impedance of 50Ω at T junction of antenna port. The important dimensional parameters to be tuned include the size of ring resonators (ar_1, ar_2, ar_3), the separation distances in between adjacent ring open loop resonator (SOLR, s_{12}, s_{23}), the feeding point of pins, the position of taping strip-line, the length(Is_1, Is_2, Is_3), width (Ws) and spacing (s_s) of coupled strip-line as well the length difference(Ia_1, Ia_2, Ia_3, Ia_4, Ia_5, Ib_1, Ib_2, Ib_3) of two strip-line connecting each BPF branch to T junction.

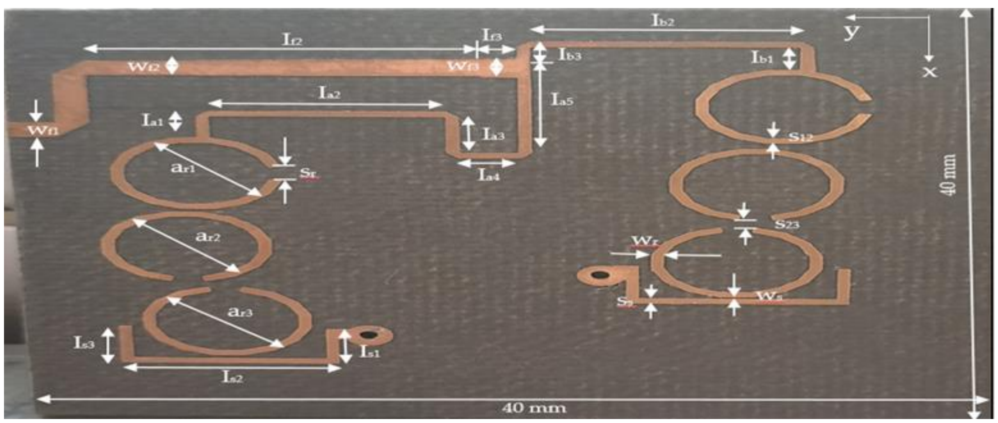

Figure 3: Top View of Strip-Line BPF Layer with Dimensions

Table 1: Dimensions of Design Antenna

ar₁	**ar₂**	**ar₃**	**bᵣ**	**sᵣ**	**wᵣ**	**s₁₂**	**s₂₃**	**sₛ**
7	7	7	7.6	1.5	0.5	0.5	0.525	0.21
Wₛ	**Is₁**	**Is₂**	**Is₃**	**t**	**Ia₁**	**Ia₂**	**Ia₃**	**Ia₄**
0.15	3.5	9	3.7	3.7	2	9.4	3.4	2.4
Ia₅	**Ib₁**	**Ib₂**	**Ib₃**	**If₂**	**If₃**	**wf₁**	**wf₂**	**wf₃**
3.4	2	10.5	1.1	11.2	2	1.35	1.47	1.73

Results and Discussion

The proposed circularly polarized BPF is experimentally designed and simulated in IE3D electromagnetic simulation software. The simulated S11 is depicted in Figure 4, in solid line where optimized design has below -14 dB and impedance bandwidth is 13.33% for passband having center frequency 4.26GHz. The S_{11} is defined for complete geometry consisting of two low pass filter circuits, phase shifter, power divider and conjugate matching circuits shown in Figure 3. The simulation radiation efficiency in the passband was more than 80% shown in Figure 8. The simulated geometry has a fourth order Chebyshev response. The (S_{11}) < -14 dB for frequency ranges from 4.1GHz to 4.8GHz. The important dimensional parameters for tuning have sizes of all SOLRs, the gap/distance in between adjacent SOLRs, the diameter of patch radiator, feed point of pins, position of tapping strip line, length, width and spacing of coupled strip line traces. Figure 4 shows simulation result for final ring resonator gives two resonance conditions at 4.26 and 4.65GHz. In Figure 5(a) rectangular resonator was used, which gives (S_{11}) < -10 dB from 3.94-4.60GHz, gives wide bandwidth, but differs from design frequency. In Figure 5(b) rectangular resonator was replaced with ring resonator and simulated for different diameters. After iterations, we finalized ring resonator design with radius 8mm, as shown in Figure 5(b), which gives less impedance bandwidth from 4.10-4.60GHz. In Figure 5(c) the position of ring resonators were changed and we got optimum results in terms of wideband from 4.1 to 4.8GHz with resonance at 4.26 and 4.65GHz. Figure 6 shows reflection coefficient comparison for rectangular, cross ring and final ring resonator design in terms of wideband, resonance conditions.

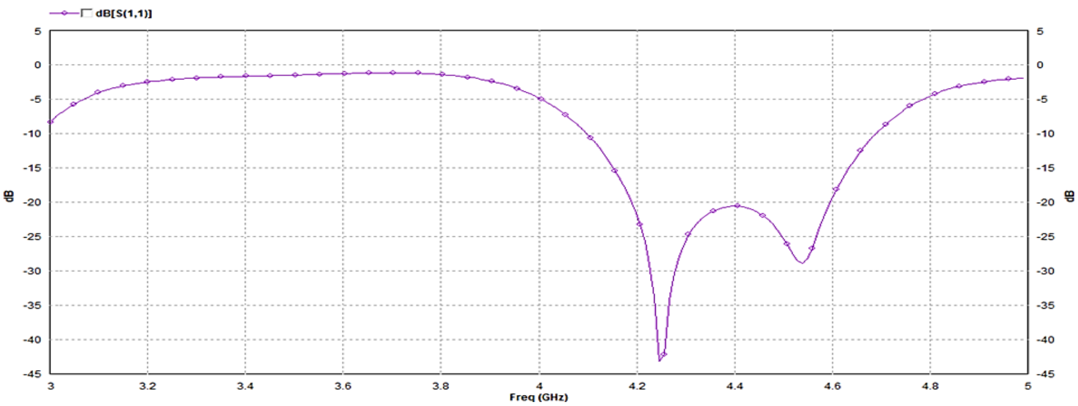

Figure 4: Simulation Result of CP Filtering Antenna Using Ring Resonator

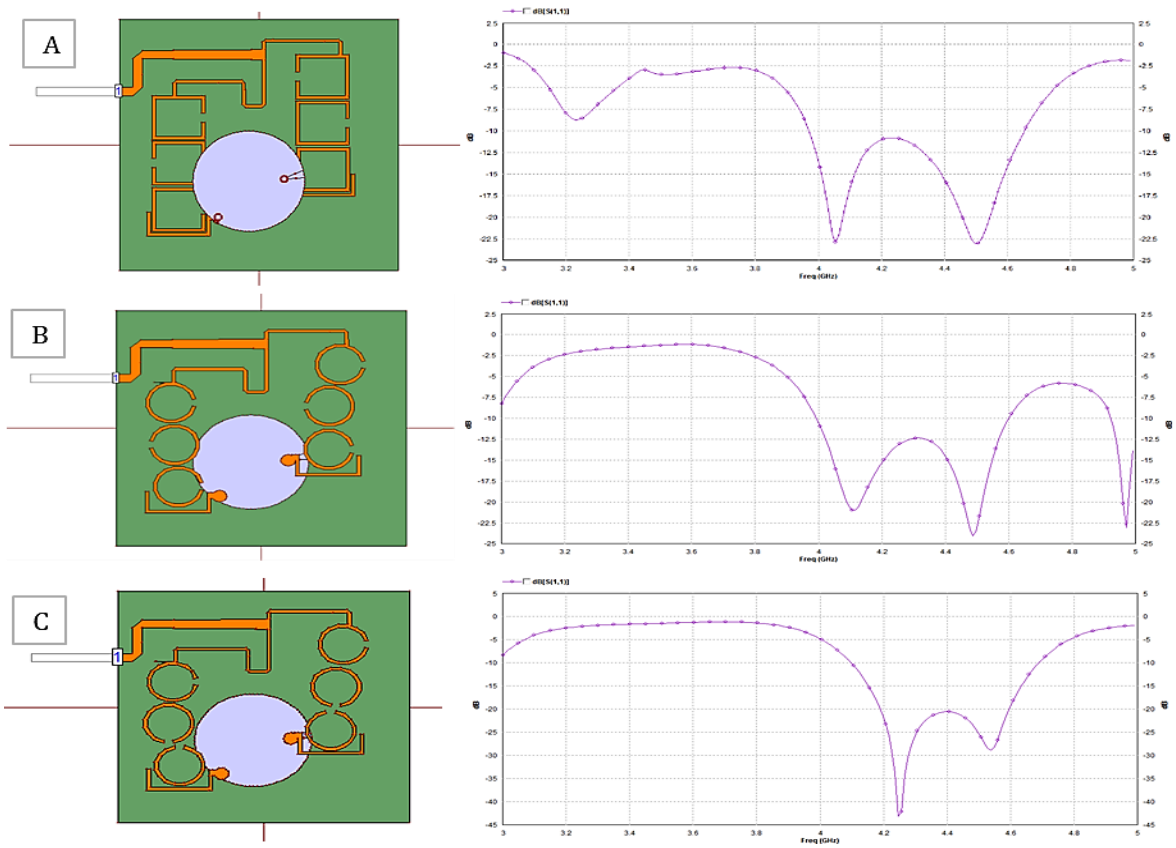

Figure 5: Simulation Result of Different Combinations (A) CP Filtering Antenna Using Rectangular Resonator, (B) CP Filtering Antenna Using Cross Ring Resonator, (C) CP Filtering Antenna with Final Ring Resonator

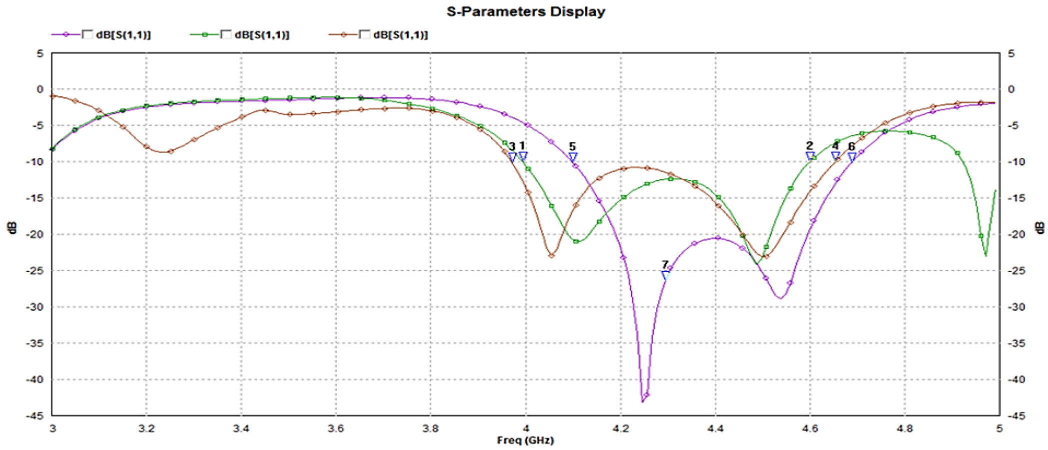

Figure 6: Simulation Results of Rectangular Resonator, Cross Ring Resonator and Final Ring Resonator Designs

If there is mismatch between two branches of low pass filter and the T junction that result in terms of increasing AR values. The AR shown in Figure 9 is less than 1dB for frequency range from frequency 3 GHz to 5GHz. For circular polarization AR value should be less than 1. Wideband CP filtenna can be obtained using other techniques using thick air substrates (41), dual feeding with planer hybrid coupler (42), broadband 90° baluns (43) and other methods in (44), but all other methods (45, 46) require more thickness. Integrating filtering and antenna may raise the size of antenna which is not compact for some wireless applications. Figure 7 shows three RT/Duroid 5880 substrate layers used for fabricating final module. The size of bottom, middle and top layers are same.

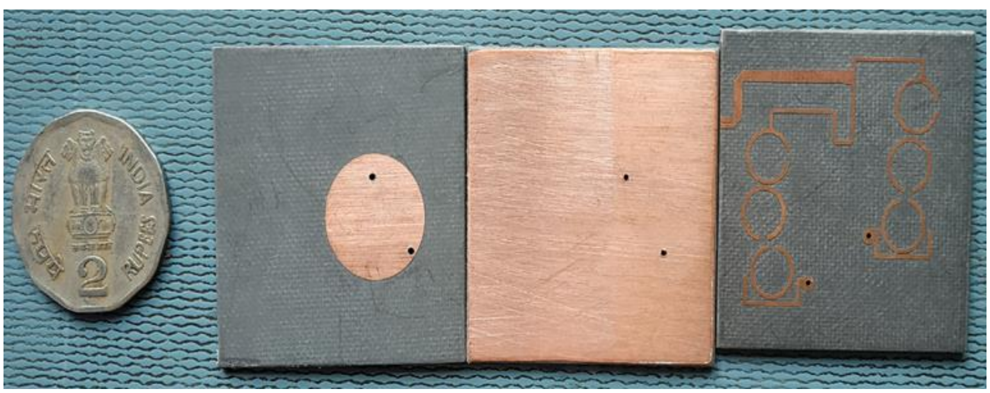

Figure 7: Three Layers of CP Filtering Antenna

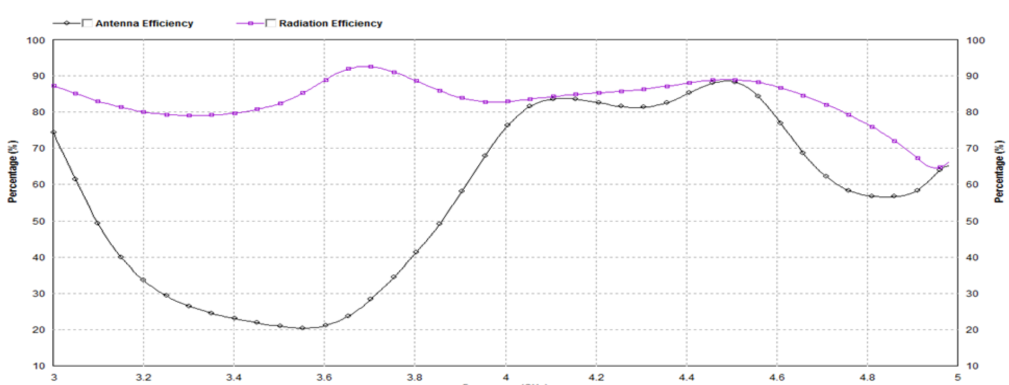

Figure 8: Efficiency of CP Filtering Antenna

Figure 8 shows radiation efficiency of CP filtering antenna which is 81.65% and antenna efficiency is 81.62% at resonance 4.26GHz and 74.98% and 77.10% at resonance frequency 4.65GHz. CP filtering antenna fabricated on RT/Duroid 5880 PCB using standard method and final prototype modules. A SMA connector was attached to planer stripline with ground terminal to both (lower and upper) ground layers. Figure 9 shows axial ratio simulation, which gives value nearer to 0.3, ideally required less than 1, which is required to obtain circular polarization.

Figure 10 shows the current distribution at 4.26GHz, at which we got resonance condition, current is non-uniformly distributed. Major current passes through left side of bandpass filter. It is seen that surface current distribution at 4.26 and 4.65GHz, the surface current density is mainly concentrated around the hybrid micro-strip coplanar waveguide in ring resonator as shown in Figure 10.

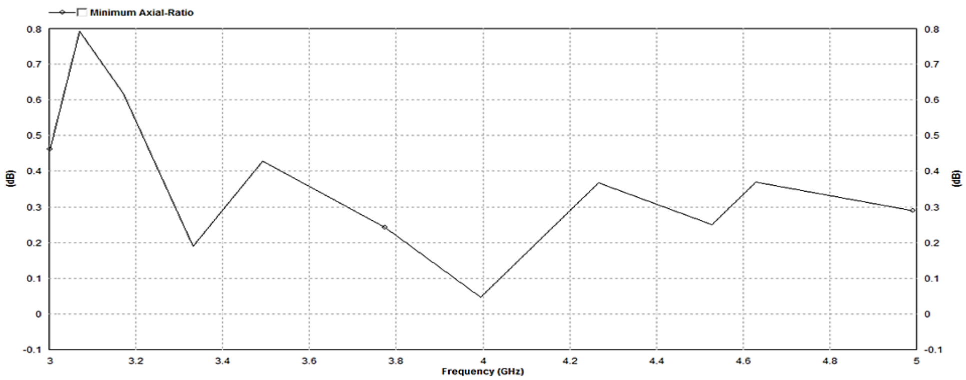

Figure 9: AR Simulation of CP Filtering Antenna

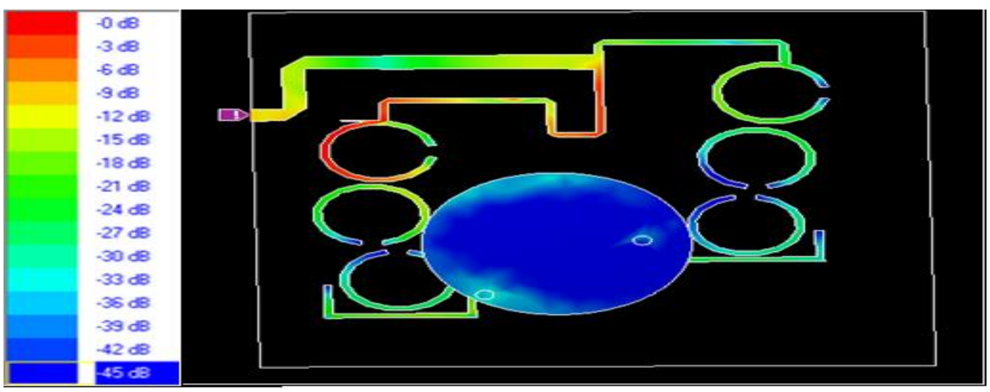

Figure 10: Current Simulation of CP Filtering Antenna at 4.26GHz

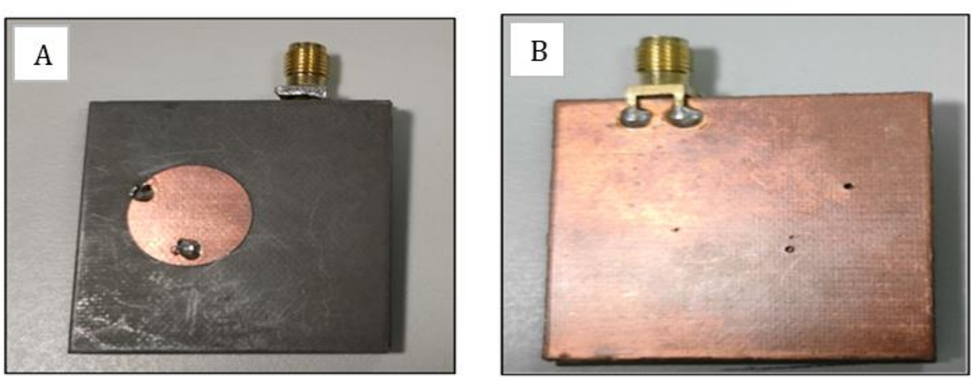

Figure 11: Photographs of Final Module (A) Top View, (B) Bottom View

Figure 11 shows photographs of top and bottom views of final fabricated and assembled CP antenna modules. A final fabricated module having bottom layer as ground layer and top layer having circular radiating patch connected to strip line filter circuit using vias. SMA connector is soldered with strip line circuit as feed point and ground terminals are connected to bottom and top layer.

RHODE and SCHWARZ ZVL network analyzer was used to measure impedance of CP filtering antennas. As shown in Figure 12 measured S_{11} of CP filtenna exhibits good filtering properties with (S_{11}) < -14dB within 4.06GHz to 4.64GHz which gives impedance bandwidth 580MHz and fractional bandwidth 13.33%. Fabrication and assembly inaccuracies can indeed cause variations between simulated and measured results, impacting parameters like S_{11} (reflection coefficient) and roll-off characteristics shifted to higher frequencies as well as broadened. Such a minor blue shift and band broadening can also be observed in measured reflection coefficient (see Figure 12). For comparison with previously reported, Table 1 includes information on footprint, antenna profile, S_{11}, pattern type, polarization, and bandwidth. The performance of this work is superior to that of previous works.

Figure 13(A) and (B) show 2D radiation pattern at 4.26GHz and 4.65GHz in both x-y and x-z patterns. Main beam is slightly shifted from broadside due to offset pin feed with respect to center of the patch and offset patch position away from center of ground plane. They have nearly equal HPBW of about 73° and 74 ° in x-y and x-z planes. The gain is nearly same (i.e.2.53dB) at 4.26GHz and 4.65GHz. The wide HPBW is favourable for angular coverage. Figure 13(C) shows 3D radiation pattern at 4.26GHz and 4.65GHz.

The normalized far-field pattern in both x-z and y-z planes shown in Figure 14. For circular polarization axial ratio (AR) should be one or less than 1. In Figure 14, purple and blue line indicates co-polarization at 4.26 and 4.65GHz respectively, and green and orange lines indicate cross polarization at 4.26 and 4.65GHz. The main beam is slightly shifted due to offset pin fed with respect to center of patch and offset patch shifted from center of ground plane. To verify performance of filtering antenna, compare previously reported antenna with antenna properties co-design, footprint, antenna profile, S_{11} bandwidth, gain, radiation efficiency, polarization and pattern in Table 2.

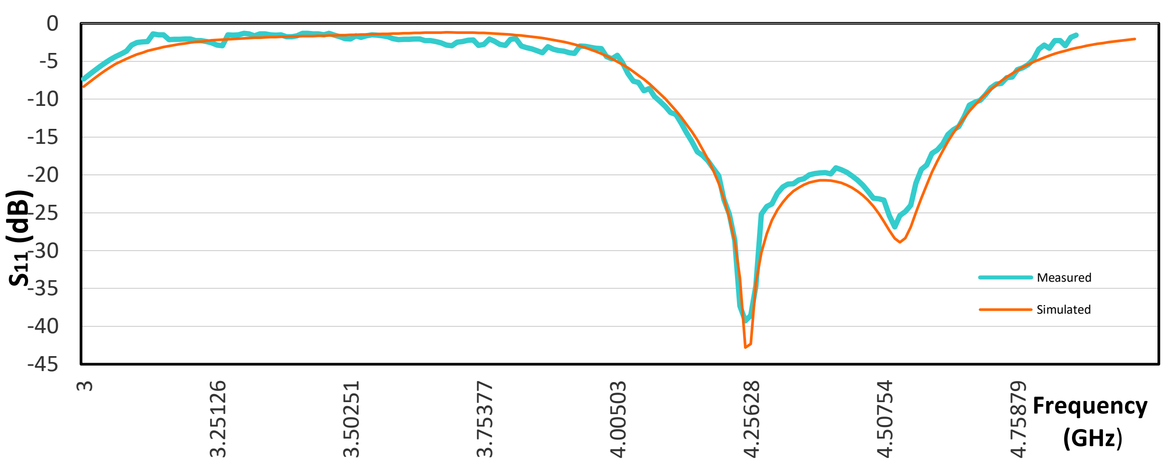

Figure 12: Simulated and Measured S11

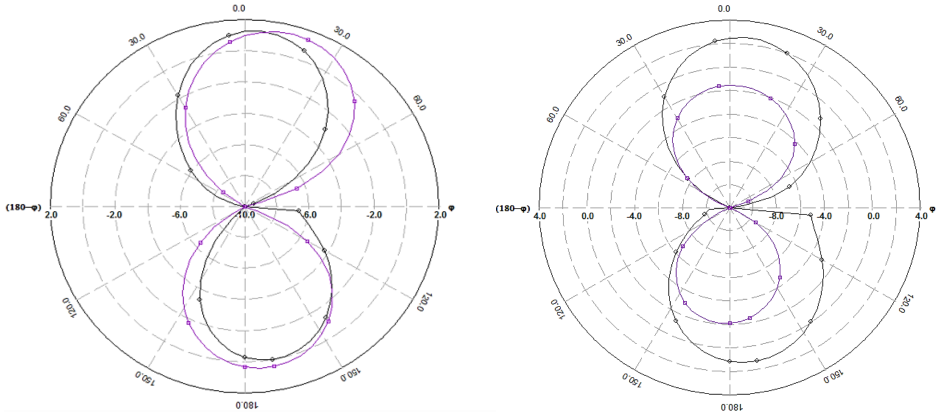

4.26GHz (A) 4.65GHz

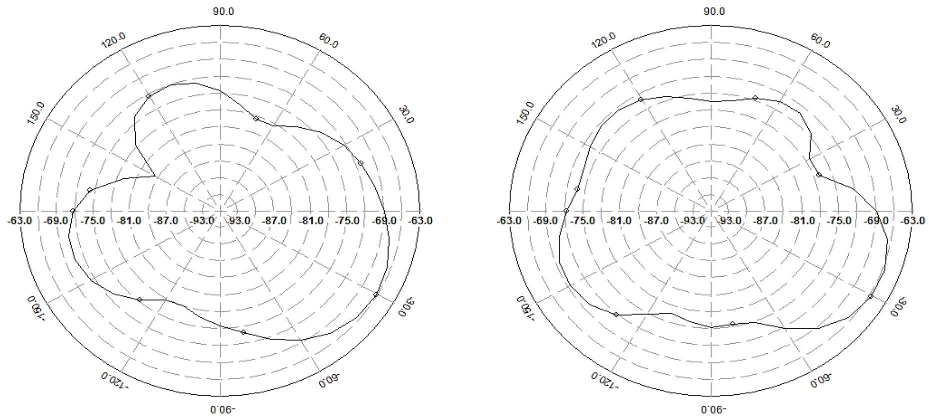

4.26GHz (B) 4.65GHz

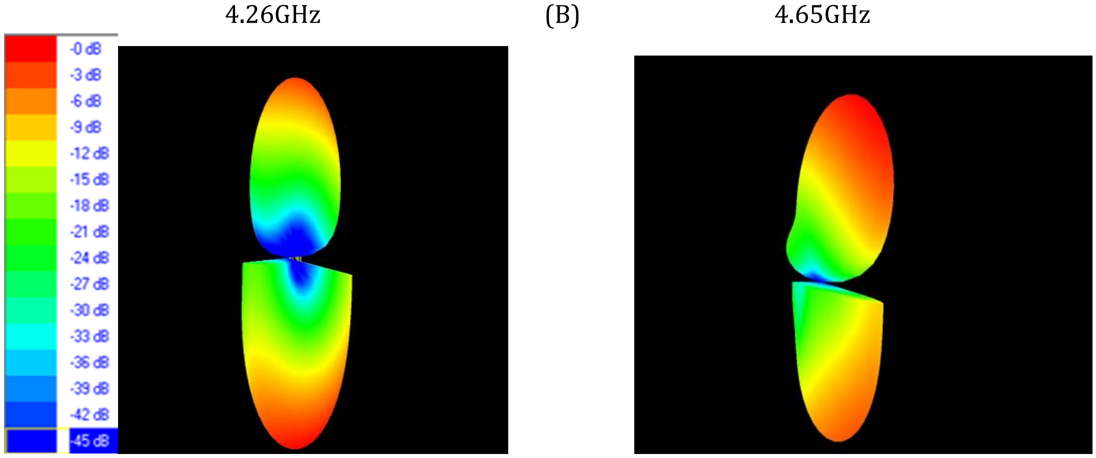

4.26GHz (C) 4.65GHz

Figure 13: Simulated 2D Radiation Pattern at (A) X-Y, (B) X-Z Plane and (C) 3D Radiation Pattern

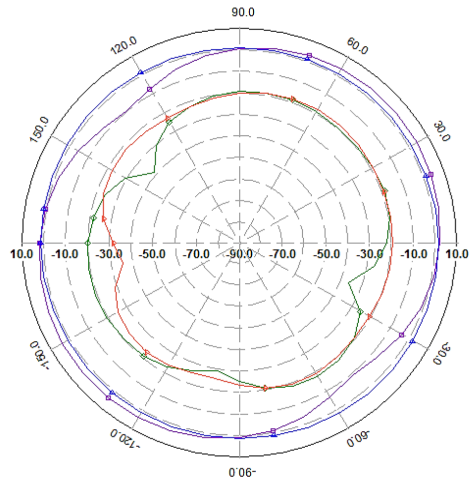

Figure 14: Co-polarization and Cross Polarization at 4.26GHz and 4.65GHz

Table 2: Performance Comparison with Other Antenna Devices

Ref	Co-design	Footprint	Profile	S_{11} BW	Gain	Rad. Efficiency	Polarization	Pattern
(4)	Yes	13.7	>3	5.5% (-13 dB)	17	50%	Linear	Highly Directive
(5)	No	3.5	>3	9.8% (-14dB)	NA	79%	Linear	Highly Directive
(6)	No	7.2	2.5	6.3% (-10dB)	14	90%	Circular	Highly Directive
(7)	No	3.01	1.7	7.7% (-10dB)	NA	74%	Linear	Omnidirectional
(8)	No	0.36	0.02	4.7% (-10dB)	4.3	50%	Linear	Unidirectional
(9)	No	0.2	0.45	4.5% (-10dB)	3.5	58%	Circular	Unidirectional
(10)	No	3.6	0.05	2.6% (-10dB)	7.8	78%	Linear	Omnidirectional
(11)	Yes	0.43	0.02	2.5% (-10dB)	4.87	NA	Linear	Unidirectional
(12)	Yes	1.56	0.1	6.1% (-15dB)	6.1	89%	Linear	Unidirectional
(13)	Yes	0.39	0.15	3% (-14dB)	4.9	59%	Linear	Unidirectional
(14)	Yes	0.32	0.01	13% (-10dB)	0.65	74%	Linear	Omnidirectional
(15)	Yes	1.17	0.01	3% (-12dB)	9.6	72%	Linear	Highly Directive
(16)	Yes	0.25	0.01	2% (-13dB)	-3	NA	Linear	Unidirectional
(47)	Yes	0.28	0.07	12.5% (-14dB)	5.2	80%	Circular	Unidirectional
(48)	Yes	0.04	0.03	8.1% (-10dB)	5.6	75%	Circular	Unidirectional
This Work	Yes	0.28	0.07	13.33% (-14dB)	2.75	81.65 %	Circular	Unidirectional

Conclusion

We proposed a novel design scheme of compact, wide impedance bandwidth CP filtenna having two LPF branches has been presented. The co-design of antenna and BPF circuit using circular radiating patch as load of open loop ring resonators. A proposed filtenna has thickness of 5.3mm and smaller size of 40mm x 40mm. A compact multiband CP filtenna operating at 4.26GHz has been designed, fabricated and validated. The proposed antenna achieves a measured S_{11}= -14dB bandwidth of 13.33% and a peak gain 2.75dBi, with AR smaller than 3dB and maximum efficiency of 81.65%. By optimizing various antenna characteristics, remarkable optimal results in comparison to the most recent literature were achieved. Measured results confirmed the proposed antenna is opponent for real time applications such as 5G applications (4.4–4.9) GHz, Unmanned aerial vehicles (4.4 to 4.5) GHz applications and (4.635 to 4.685) GHz for radar information distribution network and future scope in wearable devices for biomedical applications.

Abbreviations

Nil.

Acknowledgement

The authors wish to acknowledge the Rogers Corporation for provide RT/Duroid 5880 material and shipping at no-charge.

Author Contributions

Kiran Hilal Sonawane: Conceptualization, Methodology, Writing - Original Draft, Preparation, Data Curation, Investigation, Writing - Reviewing and Editing, Formal Analysis, Visualization; Dr. Pravin Sahebrao Patil: Supervision, Project Administration, Funding Acquisition.

Conflicts of Interest

The authors declared that there are no conflicts of interest regarding the publication of this manuscript.

Ethics Approval

Not Applicable.

Funding

No funding received for the research.

References

1. Pozar DM. Microwave and RF design of wireless systems. 2nd ed. New York, USA: Wiley; 2000..
2. Cameron RJ, Kudsia CM, Mansour RR. Microwave filters for communication systems: fundamentals, design, and applications. John Wiley and Sons: 2018;17.
3. Hong JS. Microstrip Filter for RF/Microwave Applications, 2nd ed., Wiley, Hoboken, NJ, United States, 2011.
4. Troubat M, Bila S, Thévenot M, Baillargeat D, Monédière T,Verdeyme S,Jecko B. Characterization of the interactions between a 60-GHz antenna and the human body in an off-body scenario. IEEE trans. microw. Theory Tech. 2007; 55(6):1182–1189.
5. Luo GQ, Hong W, Tang HJ, Chen JX, Yin XX, Kuai ZQ, Wu K. Filtenna consisting of horn antenna and substrate integrated waveguide cavity FSS. IEEE transactions on antennas and propagation. 2007; 55(1):92-8.
6. Barbuto M, Trotta F, Bilotti F, Toscano A. A combined bandpass filter and polarization transformer for horn antennas IEEE antennas and wireless propagation letters. 2013; 12:1065-1068.
7. Zhou H, Qu S, Lin B, Wang J, Ma H, Xu Z, Peng W, Bai P. Filter-antenna consisting of conical FSS radome and monopole antenna. IEEE Transactions on Antennas and Propagation. 2012; 60(6):3040-5.
8. Zuo J, Chen X, Han G, Li L, Zhang W. An integrated approach to RF antenna-filter co-design. IEEE Antennas and Wireless Propagation Letters. 2009; 8:141-4.
9. Jiang ZH, Gregory MD, Werner DH. Design and experimental investigation of a compact circularly polarized integrated filtering antenna for wearable biotelemetric devices. IEEE Transactions on Biomedical Circuits and Systems. 2015; 10(2):328-38.
10. Yu C, Hong W, Kuai Z, Wang H. Ku-band linearly polarized omnidirectional planar filtenna. IEEE Antennas and Wireless Propagation Letters. 2012; 11:310-3.
11. Nova OA, Bohorquez JC, Pena NM, Bridges GE, Shafai L, Shafai C. Filter-antenna module using substrate integrated waveguide cavities. IEEE Antennas and Wireless Propagation Letters. 2011; 20(10):59-62.
12. Yusuf Y, Gong X. Compact low-loss integration of high Q 3-D filters with highly efficient antennas. IEEE transactions on microwave theory and techniques. 2011; 59(4):857-65.
13. Yusuf Y, Cheng H, Gong X. A seamless integration of 3-D vertical filters with highly efficient slot antennas. IEEE Transactions on Antennas and Propagation. 2011; 59(11):4016-22.
14. Chuang CT, Chung SJ. Synthesis and design of a new printed filtering antenna. IEEE transactions on antennas and propagation. 2011; 59(3):1036-42.
15. Lin CK, Chung SJ. A filtering microstrip antenna array. IEEE transactions on microwave theory and techniques. 2011; 59(11):2856-63.
16. Lin CK, Chung SJ. A compact filtering microstrip antenna with quasi-elliptic broadside antenna gain response. IEEE Antennas and wireless propagation letters. 2011; 10:381-4.
17. Hall PS, Hao Y. Antennas and propagation for body-centric wireless communications. 2nd ed. Norwood, MA, USA: Artech house; 2012.
18. Yang GZ. Body Sensor Networks. 2nd ed. London: Springer; 2006.
19. Hall PS, Hao Y, Nechayev YI, Alomainy A, Constantinou CC, Parini C, Kamarudin MR, Salim TZ, Hee DT, Dubrovka R, Owadally AS. Antennas and propagation for on-body communication systems. IEEE Antennas and Propagation Magazine. 2007; 49(3):41-58.
20. Nechayev YI, Hall PS, Hu ZH. Characterisation of narrowband communication channels on the human body at 2.45 GHz. IET Microwaves, Antennas and Propagation. 2010; 4(6):722-32.
21. Suma MN, Bybi PC, Mohanan P. A wideband printed monopole antenna for 2.4-GHz WLAN applications. Microwave and Optical Technology Letters. 2006; 48(5):871-3.
22. Chen HD, Chen JS, Cheng YT. Modified inverted-L monopole antenna for 2.4/5 GHz dual-band operations. Electronics letters. 2003; 39(22):1567-8.
23. Wang Z, Lee LZ, Psychoudakis D, Volakis JL. Embroidered multiband body-worn antenna for GSM/PCS/WLAN communications. IEEE Transactions on Antennas and Propagation. 2014; 62(6):3321-9.

24. Soh PJ, Vandenbosch GA, Ooi SL, Rais NH. Design of a broadband all-textile slotted PIFA. IEEE transactions on antennas and propagation. 2011; 60(1):379-84.
25. Bai Q, Langley R. Crumpling of PIFA textile antenna. IEEE Transactions on Antennas and Propagation. 2011;60(1):63-70.
26. Varnoosfaderani MV, Thiel DV, Lu JW. A folded slot antenna with full ground plane for wearable waterproof wireless sensors. In2014 IEEE Antennas and Propagation Society International Symposium (APSURSI) 2014 Jul 6 (pp. 838-839). IEEE.
27. Varnoosfaderani MV, Thiel DV, Lu J. External parasitic elements on clothing for improved performance of wearable antennas. IEEE Sensors Journal. 2014; 15(1):307-15.
28. Alomainy A, Hao Y, Owadally A, Parini CG, Nechayev Y, Constantinou CC, Hall PS. Statistical analysis and performance evaluation for on-body radio propagation with microstrip patch antennas. IEEE Transactions on Antennas and Propagation. 2007; 55(1):245-8.
29. Haga N, Saito K, Takahashi M, Ito K. Characteristics of cavity slot antenna for body-area networks. IEEE Transactions on Antennas and Propagation. 2009; 57(4):837-43.
30. Agneessens S, Rogier H. Compact half diamond dual-band textile HMSIW on-body antenna. IEEE Transactions on Antennas and Propagation. 2014; 62(5):2374-81.
31. Zhu S, Langley R. Dual-band wearable textile antenna on an EBG substrate. IEEE transactions on Antennas and Propagation. 2009; 57(4):926-35.
32. Raad HR, Abbosh AI, Al-Rizzo HM, Rucker DG. Flexible and compact AMC based antenna for telemedicine applications. IEEE Transactions on antennas and propagation. 2012; 61(2):524-31.
33. Yan S, Soh PJ, Vandenbosch GA. Low-profile dual-band textile antenna with artificial magnetic conductor plane. IEEE Transactions on Antennas and Propagation. 2014; 62(12):6487-90.
34. Jiang ZH, Brocker DE, Sieber PE, Werner DH. A compact, low-profile metasurface-enabled antenna for wearable medical body-area network devices. IEEE Transactions on antennas and propagation. 2014; 62(8):4021-30.
35. Hertleer C, Rogier H, Vallozzi L, Van Langenhove L. A textile antenna for off-body communication integrated into protective clothing for firefighters. IEEE transactions on antennas and propagation. 2009; 57(4):919-25.
36. Kaivanto EK, Berg M, Salonen E, De Maagt P. Wearable circularly polarized antenna for personal satellite communication and navigation. IEEE Transactions on Antennas and Propagation. 2011; 59(12):4490-6.
37. Hong JS, Lancaster MJ. Couplings of microstrip square open-loop resonators for cross-coupled planar microwave filters. IEEE Transactions on Microwave theory and Techniques. 1996; 44(11):2099-109.
38. Zhu L, Sun S, Li R. Microwave bandpass filters for wideband communications. Hoboken, NJ, USA: Wiley; 2012.
39. Pozar DM. Microwave Engineering, 4th ed., Wiley, Hoboken, NJ, United States, 2011.
40. Pues HF, Van De Capelle AR. An impedance-matching technique for increasing the bandwidth of microstrip antennas. IEEE transactions on antennas and propagation. 1989; 37(11):1345-54.
41. Lau KL, Luk KM. A novel wide-band circularly polarized patch antenna based on L-probe and aperture-coupling techniques. IEEE Transactions on Antennas and Propagation. 2005; 53(1):577-82.
42. Qing XM. Broadband aperture-coupled circularly polarized microstrip antenna fed by a three-stub hybrid coupler. Microwave and optical technology letters. 2004; 40(1):38-41.
43. Guo YX, Khoo KW, Ong LC. Wideband circularly polarized patch antenna using broadband baluns. IEEE Transactions on Antennas and Propagation. 2008; 56(2):319-26.
44. Gao SS, Luo Q, Zhu F. Circularly Polarized Antennas. Hoboken, NJ, United States: Wiley; 2014.
45. Sonawane K, Patil P. Multiband Slot Antenna with DGP for Future Wireless Applications. In2022 International Conference on Industry 4.0 Technology (I4Tech) 2022 Sep 23 (pp. 1-5). IEEE.
46. Patil CS, Patil PS, Birare MU. Dual Feed Triangular Slotted Microstrip Patch Antenna. International Journal of Advanced Research in Electrical, Electronics and Instrumentation Engineering. 2013; 2(10):4833-6.
47. Jiang ZH, Werner DH. A compact, wideband circularly polarized co-designed filtering antenna and its application for wearable devices with low SAR. IEEE Transactions on Antennas and Propagation. 2015; 63(9):3808-18.
48. Tang MC, Li D, Wang Y, Hu KZ, Ziolkowski RW. Compact low-profile linearly and circularly polarized filtennas enabled with custom-designed feed-probe structures. IEEE Transactions on Antennas and Propagation.2020;68(7):5247-5256.